Experimental Results with HF Underwater Acoustic Modem for High Bandwidth Applications

James Younce, Andrew Singer, Thomas Riedl, Blake Landry, Andrew Bean and Toros Arikan
University of Illinois at Urbana-Champaign, 1308 West Main St. Urbana, IL 61801, USA

***Abstract*—We present a robust, video-capable modem designed for wireless underwater acoustic communication. The difficult nature of the underwater acoustic channel necessitates explicit Doppler compensation and mitigation of severe multipath. Due to the relatively low propagation speed of sound in water, platform mobility causes severe Doppler that cannot be treated as in RF wireless communicaiton, as a frequency shift or through a global rescaling. We model the underwater acoustic channel with explicit time-varying Doppler and multipath, and derive the turbo resampling equalizer (TRE) that tracks and mitigates these phenomena. Building on previous work, we demonstate experimental results achieving data rates in excess of 1 Mbps over 100 m in shallow water, and successfully transmit live video over a 5 m underwater acoustic channel from a rapidly moving transmitter with speeds in excess of $3\,\mathrm{m/s}$ and accelerations in excess of $7\,\mathrm{m/s}^2$.**

I. Introduction

Equalization methods with sophisticated Doppler compensation are essential elements of underwater acoustic communication systems, needed to satisfy the growing demand for high-bandwidth underwater wireless communication. Video communication plays a vital role in the operation of remotely operated vehicles (ROVs), used extensively in the oil and gas industry. Due to limitations in existing wireless acoustic communication systems, ROVs must transmit such video signals through a tether, or cable, linking the vehicle to a remote operator on the surface, or at a remote site, tethered to the region of operation. This means that subsea ROVs require expensive surface vessels for their operation in the field. Autonomous underwater vehicles (AUVs) operate without human input and are only used in areas where supervisory control is minimal and there is little danger of vehicles coming in contact with subsea equipment or operations. A high-bandwidth, reliable wireless underwater modem could enable AUVs and ROVs to become "wirelessly tethered" to wireless subsea hubs, and could enable real-time control of such vehicles, with operator feedback and live-streaming video, massively reducing operational costs.

Accurate Doppler compensation is critical for wide bandwidth underwater acoustic communication. Because the propagation speed of sound in water is only 2 to 3 orders of magnitude faster than typical platform motion, such mobility introduces severe distortion in the received waveform in the form of a time-varying dilation and contraction of the acoustic signal. Using a higher carrier frequency or a wider bandwidth signal to increase data rate, futher exacerbates these effects. Hence, while substantially lower bandwidth acoustic communcation systems can model Doppler effects as a time-varying phase uncertainty in the received waveform, much higher bandwidth transmissions must employ more sophisticated means. In the experimental work presented here, we incorporate explicit Doppler estimation, tracking, and correction [1] to compensate dynamically for these effects.

We have developed a single-carrier method that uses iterative multichannel turbo equalization [2] to achieve substantial improvements over previous single-carrier Doppler compensation schemes [3], with the goal of developing a video-capable underwater modem. In prior work, we demonstrated algorithmic [4] and experimental performance [5] of a turbo resampling equalizer (TRE) in a number of controlled environments. We have recently demonstrated underwater acoustic video transmission with data rates of 2 Mbit/s over distances of 5 m, with a transmitter exhibiting substantial motion and acceleration. We have also demonstrated underwater acoustic transmission at data rates in excess of 1 Mbit/s over distances in excess of 100 m in a shallow-water environment. In this paper, we outline the design and performance of this single-carrier TRE. We provide a model for wideband, short range underwater acoustic communication in the presence of motion to derive the TRE method, and then present an overview of the equalizer's operation. We finally present our newest experimental results in detail.

The paper is organized as follows. Section II discusses Doppler compensation methods for underwater acoustic communications. In Section III a channel model for the UWAC is shown that takes time-varying attenuation, noise, and multipath effects into account. Section IV outlines the single-carrier adaptive resampling equalizer and Section V presents experimental results. Section VI concludes the paper.

II. Previous Work

Underwater acoustic communication that is immune to Doppler is possible, but at the expense of arbitrarily low spectral efficiency and data rate. The first underwater acoustic digital modems employed frequency-shift keying (FSK), where guard intervals between consecutive tones ensured that reverberation did not correlate them, and guard bands guaranteed that Doppler shifts did not cause misinterpretation at the receiver. Underwater modems using this technique typically had data rates of less than 1 kbps [6].

In the 1990s, it was demonstrated that acoustic propagation allows phase-coherent underwater digital communication [7]. The authors combined an adaptive linear decision feedback equalizer (DFE) and a phase locked loop (PLL) to combat the channel distortion due to reverberation and Doppler effects. This system was evaluated in the field, and achieved a data rate of 10 kbps in shallow water over a distance of 3.7 km using 5 kHz of bandwidth, a stationary 183 dB SPL source and a stationary directional receiving element (hydrophone). This demonstrated coherent communication's potential to improve data rates and bandwidth efficiency. The directional hydrophone helped reject the noise generated at the surface due to wind and wave motion, and also limited reverberation since multipath components with the most delay generally impinge on the hydrophone at the widest angles. In a follow-up paper [8], it was recognized that the communication system devised in [7] could not handle the levels of Doppler introduced by standard mobile platforms such as autonomous underwater vehicles (AUVs). The original approach was extended with the proposition of a two-step detection algorithm. For each received data block, the detector first obtained an estimate of the average Doppler factor over the entire transmission and then resampled and phase corrected the demodulated baseband signal based on this factor. In the second step, the original method from [7] was used to estimate the data symbols. The PLL's role was to remove any residual Doppler distortion from the demodulated signal, while an adaptive equalizer estimated the transmitted symbols from the Doppler-compensated signal. Data rates of up to 2.5 kbps were achieved with moving platforms at relative speeds of up to 3 m/s.

Computationally-efficient Doppler estimation techniques were used in [9] to achieve rates of 16 kbit/s with a transmitting platform moving at up to 2.6 m/s. In [10], multiple transmitters and space-time trellis codes were used to capitalize on the benefits of the transmit diversity available in the reverberant horizontal shallow-water acoustic communication channel. The highest reliably achieved data rate was 40 kbps at a bit error rate (BER) of around 10^{-2}, using four transmitters and 23 kHz of bandwidth. The transmit and receive arrays were stationary and placed 2 km apart. The source power level was set to 190 dB. In [11], two transducers were mounted onto the ends of a 10 m pole, which was then vertically submerged. The authors achieved a data rate of 150 kbps using 25 kHz of bandwidth with unspecified transmit power. This translates to a bandwidth efficiency of 6 bps/Hz. In both of these studies, however, the receiver and transmitter were stationary. The main shortcoming of the above algorithms is that their applicability is restricted to scenarios with negligible Doppler spread and Doppler variation that is sufficiently small and roughly constant for the duration of a block. Motion-induced Doppler effects would have severely degraded the performance of the proposed algorithms.

Another approach to modulation in underwater acoustic communication is the use of orthogonal frequency-division multiplexing (OFDM), which makes the fundamental assumption that the channel is linear and time invariant for the length of each OFDM symbol. Platform motion and environmental fluctuations make the underwater acoustic channel highly time-variant, and the application of standard OFDM leads to communication algorithms that break down when the transmitter or receiver are mobile. While several modifications to the original OFDM receiver algorithm have been suggested and tested at sea [12], [13], [14], [15], [16] these methods still assume that Doppler variation is sufficiently small and roughly constant for the duration of an OFDM symbol, making such methods only applicable in low bandwidth applications. Two other approaches to mitigating the inter-carrier interference (ICI) induced due to the non-orthogonality of OFDM in time-varying evironments are presented in [17]. One method extends the channel model to include ICI due to the closest two subcarriers, while the other makes use of decision-feedback equalization (DFE) [18] and a second-order phase-locked loop. These methods make the OFDM system more robust to Doppler effects for mobile platforms, performing about as well as PLL-based single carrier methods. The enhanced OFDM schemes do not account for the possibility of different propagation paths having different Doppler. This problem is tackled in [19], [20], [21], yielding improved BER over prior single-resampling OFDM methods.

III. Channel Model

The underwater acoustic channel is one of the most difficult channels [1], [22] for digital communicaiton. When an acoustic signal is emitted at some location and acoustic measurements are taken at some other sufficiently close location, the measurements contain information about the emitted signal but are also distorted by motion, frequency-selective attenuation, multipath propagation and noise. Unlike in mobile radio systems on land, motion-induced Doppler effects cannot be neglected in underwater acoustic communication systems because the wave propagation speed is five orders of magnitude slower, 1500 m/s compared to 3×10^8 m/s.

In this section, we introduce a channel model for mobile acoustic communication that builds upon the established physical principles of acoustic wave propagation. We then derive a communication algorithm that is robust to realistic levels of Doppler in Section IV. As a first step, we consider acoustic signal propagation in an ideal fluid without attenuation, reflective boundaries or noise. There is only a single propagation path between the transmitter at $\boldsymbol{x}_{tx}(t)$ and the receiver at $\boldsymbol{x}_{rx}(t)$. The transmitter emits the acoustic signal $\tilde{s}(t)$ and the receiver senses the signal $\tilde{r}(t)$. For subsonic movement of the transmitter and receiver, the far field solution at $\boldsymbol{x}_{rx}(t)$ is

$$p^{FF}\left(\boldsymbol{x}_{rx}(t), t\right) = \frac{\left(\frac{\partial t_e}{\partial t}\right)^2}{\left\|\boldsymbol{x}_{rx}(t) - \boldsymbol{x}_{tx}(t_e)\right\|} \tilde{s}_1(t_e) \qquad (1)$$

where t_e is the unique solution to the implicit equation

$$t - t_e - \frac{\left\|\boldsymbol{x}_{rx}(t) - \boldsymbol{x}_{tx}(t_e)\right\|}{c} = 0 \qquad (2)$$

[23], and is called the emission time, with the Euclidean norm being used. The value of $\frac{\partial t_e}{\partial t}$ is always positive and equal to unity when there is no motion, greater than 1 when the source and receiver are moving towards each other and smaller than 1 otherwise. When the transmitter trajectory $\boldsymbol{x}_{tx}(t)$ is

differentiable with $\|\dot{\boldsymbol{x}_{tx}}(t)\| < c$, there exists a unique solution t_e to Equation (2) that may be obtained using a fixed-point iteration algorithm [24]. Neglecting the near field component of the solution, the channel model becomes

$$\tilde{r}(t) = h(t)\tilde{s}(t_e) \tag{3}$$

where $h(t)$ is a real-valued function of time. Comparison with Equation (1) shows that $h(t)$ is inversely proportional to communication distance and does not depend on the transmitted signal. For these reasons we refer to $h(t)$ as the channel gain. We expand the basic model in Equation (3) by successively adding frequency-selective attenuation, ambient Gaussian noise with a colored spectrum, and multipath effects [24]. The resulting received signal becomes

$$\tilde{r}(t) = \sum_p \int_\tau h_p(t,\tau)\tilde{s}(t_p(t) - \tau)\, d\tau + \tilde{v}(t) \tag{4}$$

where t_p is the unique solution to the implicit equation

$$t - t_p - \frac{\|\boldsymbol{x}_{rx}(t) - \boldsymbol{x}_{tx;p}(t_p)\|}{c} = 0 \tag{5}$$

with $\boldsymbol{x}_{tx;p}(t)$ denoting the position of the p-th hypothesized phantom source projecting arrival paths through a reflection boundary and $h_p(t,\tau)$ denoting the time-varying signal attenuation kernel along the path from the pth phantom source to the receiving transducer. Note that when there is multipath, we interpret each path as the line of sight (LOS) path from a phantom source at position $\boldsymbol{x}_{tx;p}(t)$ sending out the same signal. The integer P counts the number of paths present between the source and the receiver.

IV. Signal Design

We transmit a sequence of symbols from a finite set of signal constellation points $\mathrm{A} \subset \mathbb{C}$, typically a QAM constellation. To this end, the sequence $s[n]$ is mapped to a continuous waveform $s(t)\colon \mathbb{R} \to \mathbb{C}$

$$s(t) = \sum_l s[l]p(t - lT) \tag{6}$$

using a basic pulse $p(t)$ time-shifted by multiples of the symbol period T. The pulse $p(t)$ is often assumed to have a bandwidth of no more than $1/T$, though a pulse shape with bandwidth expansion by a factor of less than 2 is also common. If some of these symbols are unknown, they can usually be assumed to be i.i.d., because the underlying bits have either been optimally compressed or randomly interleaved. This signal is then modulated to passband

$$\tilde{s}(t) = \sqrt{2}\Re\{s(t)e^{j2\pi f_C t}\} \tag{7}$$

at carrier frequency f_C. At the receiver, the signal $\tilde{r}(t)$ from Equation (4) is demodulated by f_C and low-pass filtered, yielding

$$r(t) = \sum_p \int_\tau h_p(t,\tau)e^{j2\pi f_C(t_p(t) - \tau - t)}s(t_p(t) - \tau)d\tau + v(t) \tag{8}$$

where $v(t)$ denotes the demodulated and filtered noise process.

The rapidly time-varying nature of the channel poses significant challenges to high-rate underwater communication. Sample-by-sample Doppler compensation is critical to enabling high bandwidth. To reliably estimate the transmitted symbols $s[n]$ from the signal $r(t)$ measured at the receiver, an adaptive resampling method, with the sampling rate adapted in real time is used. We first consider the case of a single propagation path between transmitter and receiver. In order to equalize the dispersion introduced by the kernel $h(t,\tau)$, to compensate the Doppler distortion as controlled by the emission time function $t_e(t)$, and to estimate the transmitted symbols $s[n]$, we dynamically resample, filter and phase-compensate the received signal. We introduce the variable $\alpha[n]$ as an estimate of the inverse emission time $t_e^{-1}(nT)$ and use an estimator of the following form to obtain estimates $\hat{s}[n]$ of the symbols $s[n]$:

$$\hat{s}[n] = e^{-2\pi j f_C(nT - \alpha[n])} \sum_{l \in [-L_{ac}:L_c]} w[n,l]^\star r(\alpha[n] - lT/2) \tag{9}$$

The equalizer weights $w[n,l]$ and sampling times $\alpha[n]$ are the variables of the estimator and are initially learned on a sequence of known symbols, and then updated in a decision-directed mode. The integers L_{ac} and L_c specify the number of anti-causal and causal taps of the equalizer, respectively. Our learning algorithm chooses the estimator variables such that the error

$$E[n] = |s[n] - \hat{s}[n]|^2 \tag{10}$$

is minimized. The sequence $\alpha[n]$ is strictly increasing and exhibits a rate of change of

$$(1 + v[n]/c)T \tag{11}$$

where $v[n]$ is the relative speed between transmitter and receiver at time nT. Since this rate of change can be significant, a higher order tracking algorithm for $\alpha[n]$ is used. The equalizer weights $w[n,l]$ can be learned by a first-order learning algorithm such as the LMS algorithm. When there are multiple paths to the receiver, each with different Doppler, the estimator from Equation (9) is extended such that each path is dynamically resampled, filtered and phase compensated.

V. Experimental Results

Our turbo resampling equalizer was used in the Mobile Acoustic Communications Experiment (MACE), achieving data rates of 39 kbps at a distance of 2.7 km and 23.4 kbps at 7.2 km distance in a shallow oceanic setting with a mobile platform [25]. Using a 64-QAM constellation, a data rate of 1.2 Mbps was achieved over 12m distances in a short-range, high-frequency testbed in an indoor flume on the UIUC campus, shown in Figure 1 [5]. An ultra-short range experiment in a smaller tank was conducted with high-frequency ultrasound transducers, with a bandwidth of 20 MHz and a center frequency of 20 MHz, transmitting 64-QAM

Fig. 1. Our short-range high-frequency acoustic communication testbed: a $1.22\text{m} \times 1.83\text{m} \times 49\text{m}$ flume.

symbols over distances of less than 1 m, achieved data rates of 120 Mbps.

More recently, field tests were conducted at a North Champaign lake site shown in Figure 2, transmitting uncoded 16-QAM symbols over approximately 107 m. The receiver processing was adjusted for the highly reverberant shallow water environment. The transmit transducer was positioned at the northwest corner of the lake, while the receive array was placed at the southern edge of the east bank. Using 250 kHz of acoustic bandwidth, rates of 1 Mbps were transmitted and successfully received and decoded. The received signal constellation is presented in Figure 3, including both a scatter plot and density estimate of the received symbols after equalization.

Fig. 2. Aerial view of the North Champaign lake site, with 100 m transmission.

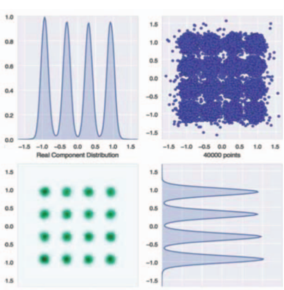

Fig. 3. Received signal constellation for the lake experiment.

We have extended our experimental apparatus for indoor measurements by constructing a motion machine overhanging a tank in the Hydrosystems laboratory at UIUC. Figure 4 illustrates the experimental setups for the the margins tank with the overhanging motion machine. This setup allowed us to test the TRE in the presence of motion-induced Doppler, moving the transmitter at up to 3 m/s with accelerations of up to 7 m/s^2. The transmitter and receiver were separated by 1 m to 5 m and QPSK symbols were transmitted with 1 MHz of acoustic bandwidth (600 kHz to 1.6 MHz). A raw effective data rate of 2 Mbps was achieved at 5 m, allowing us to transmit real-time streaming video. Figure 5 shows the velocity estimate recovered from the received signal for this particular experiment, and Figure 6 shows the successfully equalized signal constellation, including the scatter plot and density estimate of the received symbols.

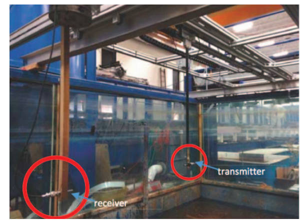

Fig. 4. Photo of motion simulator installed over the margins gank.

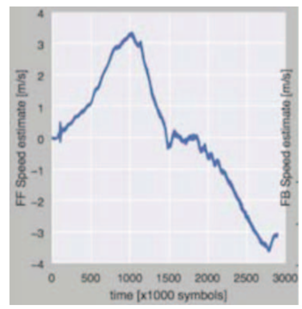

Fig. 5. Velocity estimate recovered from the received signal.

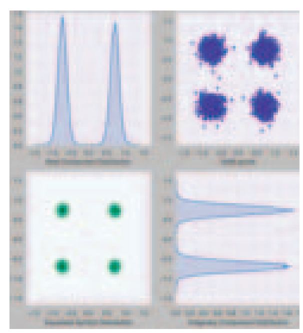

Fig. 6. Received signal constellation for the motion machine experiment.

VI. Conclusion

In this paper, we have outlined the design and performance of a turbo resampling equalizer for high bandwidth underwater acoustic communication. We provided a channel model for underwater communications that takes platform motion, time-varying attenuation, noise, and multipath effects into account and outlined an algorithm for resampling and equalization that can be extended to arrays of transducers and can cope with motion-induced Doppler. Experimental results are shown for successful shallow water transmission at data rates of 1 Mbps over 100 m in a lake environment and real-time streaming video transmission from a mobile platform exhibiting accelerations in excess of $7\,\mathrm{m}/s^2$ and mobile velocities in excess of 3 m/s.

Acknowledgment

This work was supported in part by Systems on Nanoscale Information fabriCs (SONIC), one of the six SRC STARnet Centers, sponsored by MARCO and DARPA and by the National Science Foundation under grant NSF ECCS 11-01338.

References

[1] A. C. Singer, J. K. Nelson, and S. S. Kozat, “Signal processing for underwater acoustic communications,” *Communications Magazine, IEEE*, vol. 47, no. 1, pp. 90–96, 2009.

[2] J. W. Choi, T. Riedl, K. Kim, A. Singer, and J. Preisig, “Adaptive linear turbo equalization over doubly selective channels,” *Oceanic Engineering, IEEE Journal of*, vol. 36, no. 4, pp. 473 –489, oct. 2011.

[3] T. J. Riedl and A. C. Singer, “Broadband doppler compensation: Principles and new results,” *Proceedings of the Forty-Fifth Asilomar Conference on Signals, Systems and Computers*, November 2011.

[4] e. a. I. . Arikan, Toros, “"comparison of ofdm and single-carrier schemes for doppler tolerant acoustic communications.",” in *OCEANS 2015-Genova*. IEEE, 2015, pp. 1–7.

[5] T. Riedl and A. Singer, “Towards a video-capable wireless underwater modem: Doppler tolerant broadband acoustic communication,” in *Underwater Communications and Networking (UComms), 2014*, Sept 2014, pp. 1–5.

[6] D. B. Kilfoyle and A. B. Baggeroer, “The state of the art in underwater acoustic telemetry,” *Oceanic Engineering, IEEE Journal of*, vol. 25, no. 1, pp. 4–27, 2000.

[7] M. Stojanovic, J. Catipovic, and J. Proakis, “Phase-coherent digital communications for underwater acoustic channels,” *Oceanic Engineering, IEEE Journal of*, vol. 19, no. 1, pp. 100 –111, jan 1994.

[8] M. Johnson, L. Freitag, and M. Stojanovic, “Improved doppler tracking and correction for underwater acoustic communications,” in *Proceedings of the 1997 IEEE International Conference on Acoustics, Speech, and Signal Processing (ICASSP ’97)*, vol. 1, 1997, pp. 575–.

[9] B. Sharif, J. Neasham, O. Hinton, and A. Adams, “A computationally efficient doppler compensation system for underwater acoustic communications,” *Oceanic Engineering, IEEE Journal of*, vol. 25, no. 1, pp. 52–61, Jan 2000.

[10] S. D. Roy, T. McDonald, and J. V. Proakis, “High-rate communication for underwater acoustic channels using multiple transmitters and spacetime coding: Receiver structures and experimental results,” *IEEE J. Oceanic Eng.*, vol. 32, pp. 663–688, July 2007.

[11] C. Pelekanakis, M. Stojanovic, and L. Freitag, “High rate acoustic link for underwater video transmission,” in *OCEANS 2003. Proceedings*, vol. 2. IEEE, 2003, pp. 1091–1097.

[12] M. Stojanovic, “Low complexity OFDM detector for underwater acoustic channels,” in *OCEANS 2006*. IEEE, 2006, pp. 1–6.

[13] B. Li, S. Zhou, M. Stojanovic, L. Freitag, and P. Willett, “Multicarrier communication over underwater acoustic channels with nonuniform doppler shifts,” *Oceanic Engineering, IEEE Journal of*, vol. 33, no. 2, pp. 198–209, 2008.

[14] B. Li, J. Huang, S. Zhou, K. Ball, M. Stojanovic, L. Freitag, and P. Willett, “Mimo-ofdm for high-rate underwater acoustic communications,” *Oceanic Engineering, IEEE Journal of*, vol. 34, no. 4, pp. 634–644, 2009.

[15] B. Li, S. Zhou, M. Stojanovic, L. Freitag, and P. Willett, “Non-uniform doppler compensation for zero-padded ofdm over fast-varying underwater acoustic channels,” in *OCEANS 2007-Europe*. IEEE, 2007, pp. 1–6.

[16] B. Li, S. Zhou, M. Stojanovic, and L. Freitag, “Pilot-tone based zp-ofdm demodulation for an underwater acoustic channel,” in *OCEANS 2006*. IEEE, 2006, pp. 1–5.

[17] K. Tu, D. Fertonani, T. Duman, M. Stojanovic, J. Proakis, and P. Hursky, “Mitigation of intercarrier interference for ofdm over time-varying underwater acoustic channels,” *Oceanic Engineering, IEEE Journal of*, vol. 36, no. 2, pp. 156–171, April 2011.

[18] I. Proakis, *Digital Communications, 4th Edition*. McGraw-Hill, New York, 2001.

[19] K. Tu, T. Duman, M. Stojanovic, and J. Proakis, “Multiple-resampling receiver design for ofdm over doppler-distorted underwater acoustic channels,” *Oceanic Engineering, IEEE Journal of*, vol. 38, no. 2, pp. 333–346, April 2013.

[20] K. Tu, T. Duman, J. Proakis, and M. Stojanovic, “Cooperative mimo-ofdm communications: Receiver design for doppler-distorted underwater acoustic channels,” in *Signals, Systems and Computers (ASILOMAR), 2010 Conference Record of the Forty Fourth Asilomar Conference on*, Nov 2010, pp. 1335–1339.

[21] J. Huang, S. Zhou, and Z. Wang, “Performance results of two iterative receivers for distributed mimo ofdm with large doppler deviations,” *Oceanic Engineering, IEEE Journal of*, vol. 38, no. 2, pp. 347–357, April 2013.

[22] M. Stojanovic and J. Preisig, “Underwater acoustic communication channels: Propagation models and statistical characterization,” *Communications Magazine, IEEE*, vol. 47, no. 1, pp. 84–89, 2009.

[23] S. Rienstra and A. Hirschberg, “An introduction to acoustics,” *Report IWDE*, pp. 92–06, 2001.

[24] T. Riedl, “Communication and time distortion,” Ph.D. dissertation, University of Illinois at Urbana-Champaign, 2014.

[25] T. Riedl and A. Singer, “Must-read: Multichannel sample-by-sample turbo resampling equalization and decoding,” in *OCEANS - Bergen, 2013 MTS/IEEE*, June 2013, pp. 1–5.